Journal of Solid State Chemistry **157,** 186–192 (2001)
doi:10.1006/jssc.2000.9074, available online at http://www.idealibrary.com on IDEAL®

A New Three-Dimensional Incommensurately Modulated Cubic Phase (in ZrP_2O_7) and Its Symmetry Characterization via Temperature-Dependent Electron Diffraction

R. L. Withers,*,[1] Y. Tabira,* J. S. O. Evans,† I. J. King,† and A. W. Sleight‡

*Research School of Chemistry, Australian National University, Canberra, A.C.T, 0200 Australia; †Department of Chemistry, Durham University, Durham, United Kingdom; and ‡Department of Chemistry, Oregon State University, Corvallis, Oregon 97331

Received August 29, 2000; in revised form November 21, 2000 accepted December 8, 2000

A detailed electron diffraction study has been made of the ZrP_2O_7 member of the AM_2O_7 family of framework structures and of its temperature-dependent structural phase transformations. The room-temperature phase corresponds to a primitive 3×3×3 superstructure phase of probable space group symmetry $Pa\bar{3}$. An observed glide extinction condition when viewed down $\langle 001 \rangle$ axes could, however, also be compatible with resultant *Pbca* space group symmetry. The high-temperature phase corresponds to the normal unmodulated parent structure. An intervening intermediate phase that exists over a relatively narrow temperature window (~ 5–10°C) around 294°C is shown to be a three-dimensional incommensurately modulated cubic phase characterized by incommensurate primary modulation wave vectors in the close vicinity of 0.31 $\langle 100 \rangle$* and probable superspace group symmetry *P*: $Pa\bar{3}$: $Ia\bar{3}$. © 2001 Academic Press

Key Words: **3-D incommensurately modulated; framework structure; phase transitions.**

1. INTRODUCTION

There exists a large family of cubic $A^{IV}M_2^{V}O_7$ compounds (A = Si, Ge, Sn, Ti, Zr, Hf, Mo,W, Re, Ce …; M = P, V, As) whose ideal (usually high temperature) parent structure (space group symmetry $Pa\bar{3}$, $Z = 4$) is built out of corner-connected AO_6 octahedra and nominally linear M_2O_7 (pyrophosphate, pyrovanadate, or pyroarsenate) units (in turn built out of two corner-connected MO_4 tetrahedra), as shown in Fig. 1 (1–5). Low isotropic thermal expansion above a normal to $3 \times 3 \times 3$ superstructure phase transition (which usually occurs above room temperature and in the range of 100–400°C (1–5)) has generated much recent interest in this family of compounds.

In the ideal parent structure, the M_2O_7 units all fall on 3-fold axes with the bridging oxygen ions on inversion centres. The M–O–M angles are thus all constrained to be 180° on average. Chemically, however, it is well known that the preferred value for such angles are normally in the range 130°–160° and invariably considerably less than 180° (see, for example, 2, 6). The energy gain associated with non linear (bent) M–O–M angles thus provides a driving force for structural change upon lowering of temperature and is presumed responsible for the normal to $3 \times 3 \times 3$ superstructure phase transition commonly observed in such systems (see (4) and references contained therein). The topological connectivity of the constituent semirigid octahedral and tetrahedral polyhedral units, however, leads to inherent structural frustration in that there are no zero frequency phonon modes (RUMs), allowing for the correlated rotation of the MO_4 tetrahedra and AO_6 octahedra (1, 2, 7). Rotations of the MO_4 tetrahedra necessarily cause the AO_6 octahedra to distort and viceversa, with the resultant structure dependent upon the particular pattern of rotation and the balance between the relative stiffnesses of the AO_6 octahedra and MO_4 tetrahedra in comparison to the energy gain associated with bending of the M–O–M bonds (1–5, 7).

Structural frustration of this sort has often been associated with incommensurability and indeed, in the case of ZrV_2O_7 (8), it has recently been shown that there exists an intermediate incommensurate phase sandwiched over a narrow temperature interval between the normal and $3 \times 3 \times 3$ superstructure phase. The existence of this intermediate incommensurate phase was clear from careful thermal expansion and DSC measurements, which showed the existence of two separate (apparently first order) phase transitions at 77 and 102°C. In the case of ZrP_2O_7, however, only one such phase transition (also apparently first order) is apparent from thermal expansion measurements (see Fig. 2), suggesting that there should be no intermediate incommensurate phase. Preliminary electron diffraction (ED) work, however, showed that ZrP_2O_7 does indeed have an intermediate incommensurate phase (8). The prime

[1] To whom correspondence should be addressed. Fax: (61)(2)62490750. E-mail: withers@rsc.anu.edu.au.

0022-4596/01 $35.00

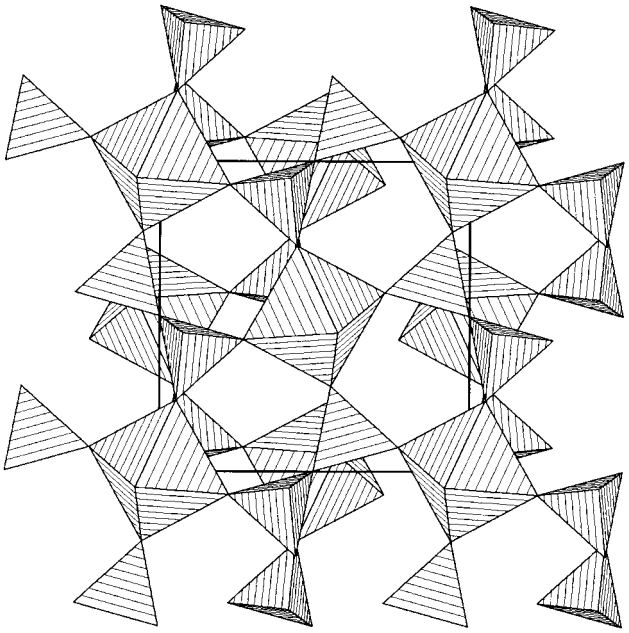

FIG. 1. The unmodulated parent structure of ZrP_2O_7 made up of corner-connected ZrO_6 octahedra and PO_4 tetrahedra projected along an $\langle 001 \rangle$ direction. The projected unit cell is outlined.

purpose of this paper is to present the results of an *in situ* electron diffraction (ED) study of this intermediate incommensurate phase.

2. EXPERIMENTAL

The synthesis of the ZrP_2O_7 used in this study is described in Refs. (1, 3). Electron microscope samples were prepared by crushing and dispersing onto holey-carbon coated molybdenum grids, which were subsequently examined in JEOL 100CX and Philips EM430 transmission electron microscopes (TEMs). The temperature-dependent ED work was carried out in the JEOL 100CX TEM using an EM-SHTH2 double tilt heating holder. The specimen tilt was very limited ($\sim \pm 3^\circ$) about the second tilt axis. This experimental constraint severely limited the ability to systematically investigate reciprocal space.

Likewise, experimental constraints limited knowledge of the exact local temperature. Local temperature depends, among other factors, on the proximity of the particular grain being investigated to the molybdenum grid bars, the thermal conductivity of the support film, the incident electron beam flux. Thus, it is not possible to know absolute temperatures at any particular grain being investigated. Notwithstanding this experimental constraint, repeated heating and cooling cycles showed that the intermediate incommensurate phase exists over a relatively narrow temperature interval ($\sim$ 5–10°C) and that both the low temperature to incommensurate and incommensurate to parent phase transitions take place close to the 294°C phase transition observed in DSC (see Fig. 2). According to the EM-SHTH2 thermocouple read-out, the latter incommensurate to high-temperature phase transition variously occurred at temperatures ranging from 285 to 305°C. It therefore seems most likely that this incommensurate to parent phase transition is the one that is observed in the DSC experiment at 294°C.

The temperature dependence of the unit cell parameters was investigated by neutron powder diffraction. Neutron diffraction data were recorded on the high-resolution powder diffractometer (HRPD) at the ISIS neutron source of the Rutherford Appleton Laboratory, U.K. Data were collected in 2°C temperature intervals from -53 to 133°C in an AS Scientific Instruments cryofurnace on 10.77 g of powdered ZrP_2O_7 packed in a 5.9-cm^3 rectangular can and from 123 to 463°C in a Rutherford furnace. Data were collected over a time-of-flight range of 34,000–114,000 μs ($d = 2.364$–0.7050 Å) for approximately 11 min at each temperature.

A temperature offset of 23°C was applied to the furnace data to match the cell parameters obtained in the cryofurnace. (The cryofurnace has individually calibrated Rh/Fe sensors, one of which sits directly on the sample, plus He exchange gas in the system to give both accurate and precise temperature readings. The Rutherford furnace, on the other hand, has type K thermocouples, which sit above and below the sample and, under vacuum operation with solely radiative heating, is much more prone to thermal gradient effects). This gave an approximate value of the phase transition temperature of 293°C. DSC gave a transition temperature of 294°C. We use the DSC-determined value of 294°C in what follows. The unit cell parameters were derived by Pawley fitting of the powder data sets using the ISIS time-of-flight Rietveld refinement program TF12LS.

3. RESULTS

As for ZrV_2O_7, the absence of sharp satellite reflections above the incommensurate to parent phase transition is consistent with a high-temperature parent, or unmodulated, phase of $Pa\bar{3}$ space group symmetry (see Fig. 1). The strong Bragg reflections corresponding to this parent structure (see Fig. 3a), and in common for all three phases, are labeled **G** in what follows. In agreement with the calculated absence of zero-frequency RUM modes in this high-temperature parent phase (1, 2, 7), there is no characteristic continuous diffuse intensity distribution accompanying the parent Bragg reflections as there is for other displacively flexible framework structures with zero-frequency RUM modes (9–11). There is, nonetheless, evidence for low-frequency Quasi-RUM (Q-RUM) modes (7, 12, 13) in the form of very weak diffuse blobs of intensity localized close to the incommensurate positions of reciprocal space at which sharp

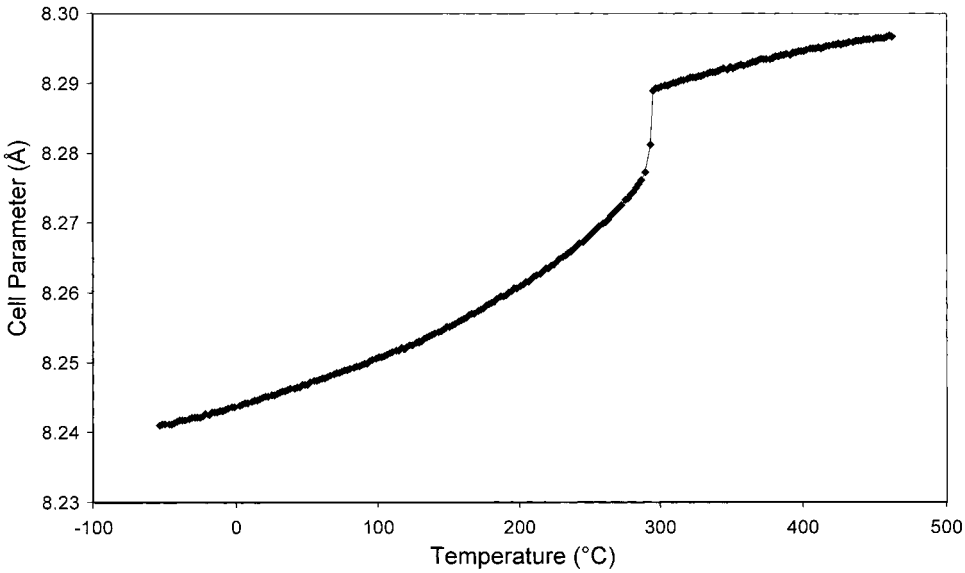

FIG. 2. Plot of the relative expansion of the low-temperature superstructure cell parameter of ZrP_2O_7 as a function of temperature. (Above 294°C, the parent cell parameter is multiplied by 3 to enable direct comparison with the low-temperature superstructure phase).

satellite reflections first condense out upon lowering through the ~ 290°C phase transition (cf., for example, the contents of the contrast-enhanced box on the left-hand side of Fig. 3a with Fig. 3b).

The reason why such Q-RUMs should necessarily have the lowest frequency (and hence be the most strongly excited) in the vicinity of these $\mathbf{G} \pm \langle \frac{1}{3}, \frac{1}{3}, 0 \rangle^*$ regions of reciprocal space or why almost all known AM_2O_7 phases have a low temperature $3 \times 3 \times 3$ superstructure phase (1–5) is not immediately apparent but the fact that the lowest frequency mode of the parent structure as output by the CRUSH lattice dynamics program always has a distinct minimum in this vicinity (see Fig. 4) suggests that the restoring force opposing polyhedral rotation for the Q-RUM is clearly minimized for modulation wave vectors in the vicinity of $\langle \frac{1}{3}, \frac{1}{3}, 0 \rangle^*$.

Again, as for ZrV_2O_7, ED results show that the low-temperature phase corresponds to a primitive $3 \times 3 \times 3$ superstructure phase (see, for example, Figs. 3c and 5a). The characteristic extinction condition ($F(hk0) = 0$ unless h is even) apparent in the zero-order laue zone (ZOLZ) region (see Fig. 3c) of $\langle 001 \rangle$ zone axis electron diffraction patterns (EDPs) of this phase necessitates the existence of an a glide and confirms the Pa portion of the $Pa\bar{3}$ space group symmetry reported for this $3 \times 3 \times 3$ superstructure phase. (Notice the doubled density of reflections along the a^* direction apparent in the first OLZ (FOLZ) ring on the right-hand side of Fig. 3c relative to that in the ZOLZ region). The only alternative possibility for the space group symmetry of this phase compatible with the observed extinction condition apparent in Fig. 3c would be orthorhombic $Pbca$ (cf., for example, with the list of possible resultant low-temperature space group symmetries given in Fig. 4 of (1)). Experimentally, however, there is no evidence for broken cubic metric symmetry in the low-temperature phase.

The intermediate incommensurate phase that exists for a narrow temperature interval (~ 5–10°C) close to (presumably immediately below) the 294°C phase transition apparent in thermal expansion and DSC experiments is characterized by incommensurate satellite reflections, by far the strongest of which fall in the close vicinity of the $\mathbf{G} \pm \frac{1}{3} \langle 110 \rangle^*$ regions of reciprocal space (see, for example, Figs. 3b and 5b), at $\mathbf{G} \pm 0.31 \langle 110 \rangle^*$. This is again rather similar to what happens in the incommensurate phase of ZrV_2O_7 (8). Unlike for ZrV_2O_7, however, in the current case the existence of this intermediate incommensurate phase is not apparent from thermal expansion and DSC experiments nor is there is ever any evidence for broken cubic $m\bar{3}$ point group symmetry. The six integer indexation of the $\langle 001 \rangle$ and $\langle 210 \rangle$ zone axis EDPs in Figs. 3b and 5b is thus with respect to the six basis vectors $\{\mathbf{a}^*, \mathbf{b}^*, \mathbf{c}^*, \mathbf{q}_1 = 0.31\mathbf{a}^*, \mathbf{q}_2 = 0.31\mathbf{b}^*, \mathbf{q}_3 = 0.31\mathbf{c}^*\}$. A reflection indexed as $hklmnp$ therefore corresponds to the $h\mathbf{a}^* + k\mathbf{b}^* + l\mathbf{c}^* + m\mathbf{q}_1 + n\mathbf{q}_2 + p\mathbf{q}_3 \equiv (h + 0.31m)\mathbf{a}^* + (k + 0.31n)\mathbf{b}^* + (l + 0.31p)\mathbf{c}^*$ reciprocal space position etc. (Such (3 + 3)-dimensional incommensurately modulated structures are extremely rare in the literature, although there have been several recently reported examples (14–16), particularly in bismuth oxide based compounds).

From a modulation wave point of view, the (primitive) primary modulation wave vectors $m\mathbf{q}_1 + n\mathbf{q}_2 + p\mathbf{q}_3$ ($m + n + p = 2J$, J an integer) characteristic of this intermediate incommensurate phase are of $\sim 0.31 \langle 110 \rangle^*$ type. Given cubic parent symmetry, there are six such

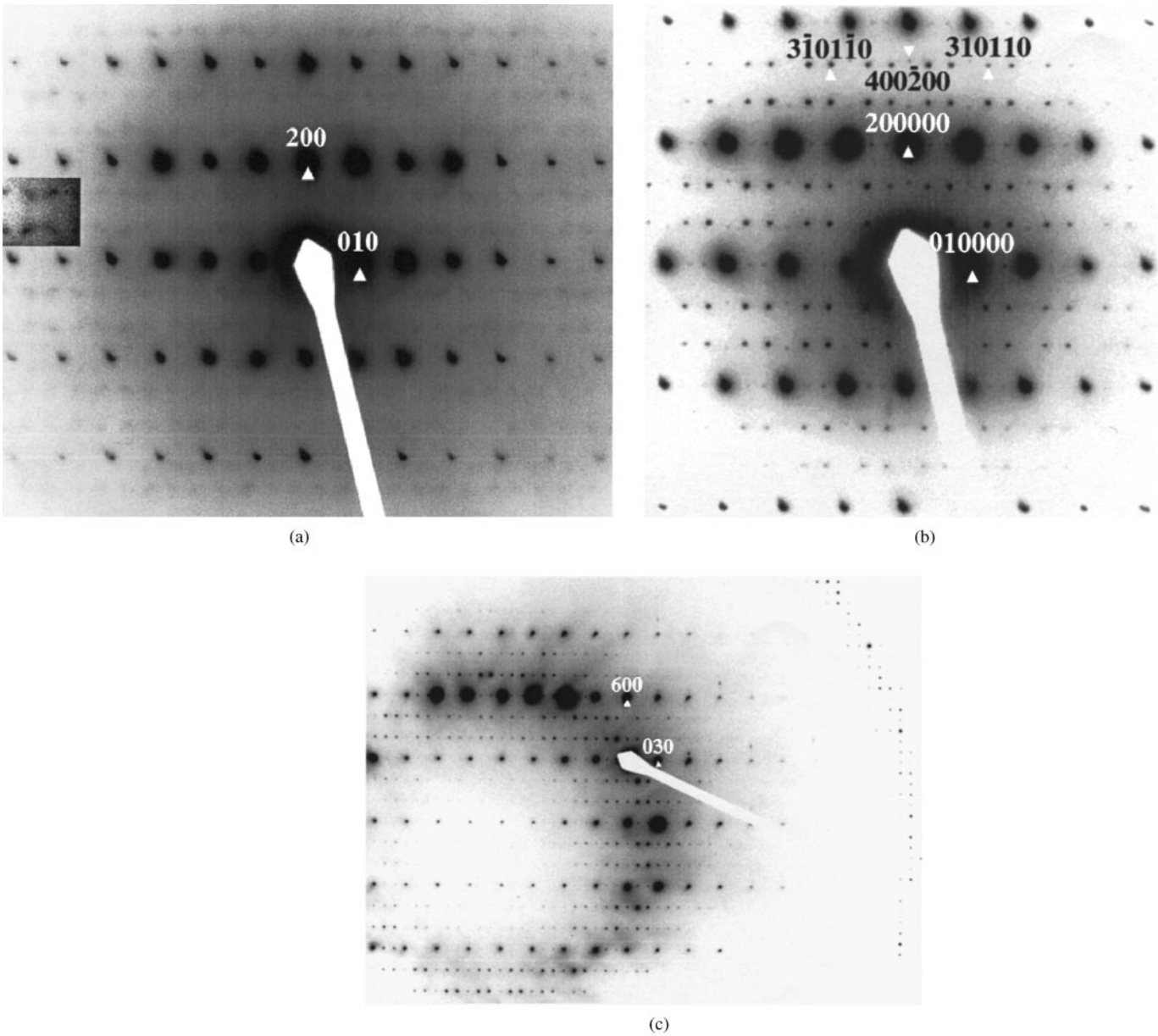

FIG. 3. Shows $\langle 001 \rangle$ zone axis EDPs typical of the (a) unmodulated parent structure, (b) the intermediate incommensurate phase, and (c) the low-temperature $3 \times 3 \times 3$ superstructure phase. (c) is taken a few degrees off axis to bring up the first-order laue zone (FOLZ) ring on the right-hand size of the EDP. Note the doubled density of reflections in the FOLZ relative to the ZOLZ. The indexation in (b) is with respect to the six basis vectors $\{\mathbf{a}^*, \mathbf{b}^*, \mathbf{c}^*, \mathbf{q}_1 = 0.31\mathbf{a}^*, \mathbf{q}_2 = 0.31\mathbf{b}^*, \mathbf{q}_3 = 0.31\mathbf{c}^*\}$. Thus, a reflection indexed as $hklmnp$ occurs at the $h\mathbf{a}^* + k\mathbf{b}^* + l\mathbf{c}^* + m\mathbf{q}_1 + n\mathbf{q}_2 + p\mathbf{q}_3$ reciprocal space position, etc.

$\sim \frac{1}{3} \langle 110 \rangle^*$ displacive modulations possible. Resultant cubic $m\bar{3}$ point group symmetry for the reciprocal lattice of this intermediate incommensurate phase requires all six such displacive modulations to simultaneously co-exist. That all six such modulations do indeed locally co-exist in the case of ZrP_2O_7 is apparent from $\langle 210 \rangle$ zone axis EDPs such as Fig. 5b, for example, where $\mathbf{G} \pm \sim 0.31 \langle 110 \rangle^*$ satellite reflections of all six types are clearly simultaneously present (if not in the ZOLZ then in the first OLZ or FOLZ).

While there is no symmetry operation either along or perpendicular to the tertiary $\langle 110 \rangle$ axes of the $Pa\bar{3}$ average structure, the (primitive) primary modulation wave vectors nonetheless run exactly along the six tertiary $\langle 110 \rangle^*$ directions in reciprocal space, as is apparent from EDPs such as Fig. 6a where a mirror plane (with respect to the positions of the satellite reflections) perpendicular to one such tertiary $\langle 110 \rangle$ axis is apparent. By contrast, this "mirror" plane is clearly missing in the incommensurate phase of ZrV_2O_7

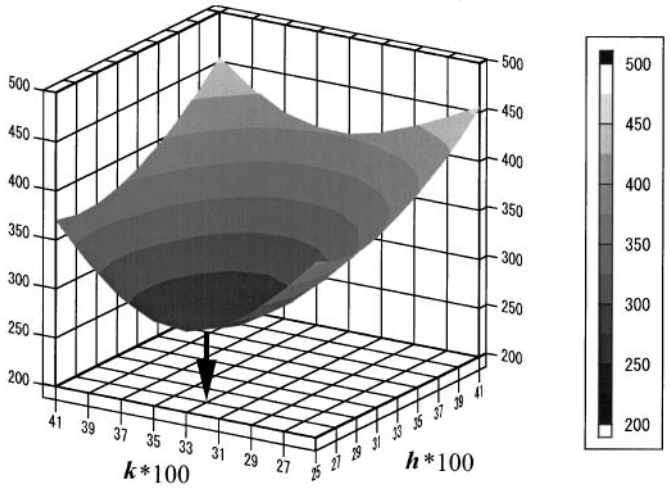

FIG. 4. Shows a contour plot of the Q-RUM frequency (arbitrary units) as output by the CRUSH lattice dynamics program. Notice the pronounced minimum in the Q-RUM frequencies for modulation wave vectors in the vicinity of $\langle \frac{1}{3}, \frac{1}{3}, 0 \rangle^*$.

(cf., Fig. 6a with Fig. 6b). Clearly, the two incommensurate phases are of quite different character and certainly not isomorphous. The reason why the presence of the incommensurate phase has not been detected via thermal expansion or DSC measurements is difficult to answer. It would appear that the maintenance of $m\bar{3}$ point group symmetry in the case of ZrP_2O_7 makes it difficult to detect the presence of the intermediate incommensurate phase.

Apart from the incommensurability of the primary modulation wave vectors, the major distinction between this intermediate incommensurate phase and the low temperature "locked-in" $3 \times 3 \times 3$ superstructure phase is, again, as for ZrV_2O_7, the significantly diminished intensity of higher order harmonic satellite reflections (such as those of $\mathbf{G} \pm \frac{1}{3}\langle 001 \rangle^*$ or $\mathbf{G} \pm \frac{1}{3}\langle 111 \rangle^*$ type) in the intermediate phase as compared to the room temperature phase (cf., for example, Fig. 3b with Fig. 3c and Fig. 5b with Fig. 5a). In the language of superspace groups, the observed extinction conditions characteristic of the intermediate incommensurate phase when indexed with respect to the six-dimensional basis set $M^* = \{\mathbf{a}^*, \mathbf{b}^*, \mathbf{c}^*, \mathbf{q}_1 = 0.31\mathbf{a}^*, \mathbf{q}_2 = 0.31\mathbf{b}^*, \mathbf{q}_3 = 0.31\mathbf{c}^*\}$ are given by $F\,[hklmnp]^* = 0$ unless $m + n + p$ is even and $F\langle hk0mn0 \rangle^* = 0$ unless $m + n$, $h + m$ are even. The former implies the existence of the superspace centering operation $\{x_1\ ,\ x_2,\ x_3,\ x_4 + \frac{1}{2},\ x_5 + \frac{1}{2},\ x_6 + \frac{1}{2}\}$ while the latter implies the presence of the hyperglide plane $\{x_1 + \frac{1}{2},\ x_2,\ -x_3 + \frac{1}{2},\ x_4 + \frac{1}{2},\ x_5,\ -x_6 + \frac{1}{2} + 2\phi_3\}$.

In conjunction with $m\bar{3}$ point group symmetry, the implied superspace group of this six-dimensional incommensurately modulated intermediate phase is $P{:}Pa\bar{3}{:}Ia\bar{3}$ ($\varepsilon\mathbf{a}^*$, $\varepsilon\mathbf{b}^*$, $\varepsilon\mathbf{c}^*$, $\varepsilon = 0.31$). The generating operations of this superspace group, in addition to the two superspace operations

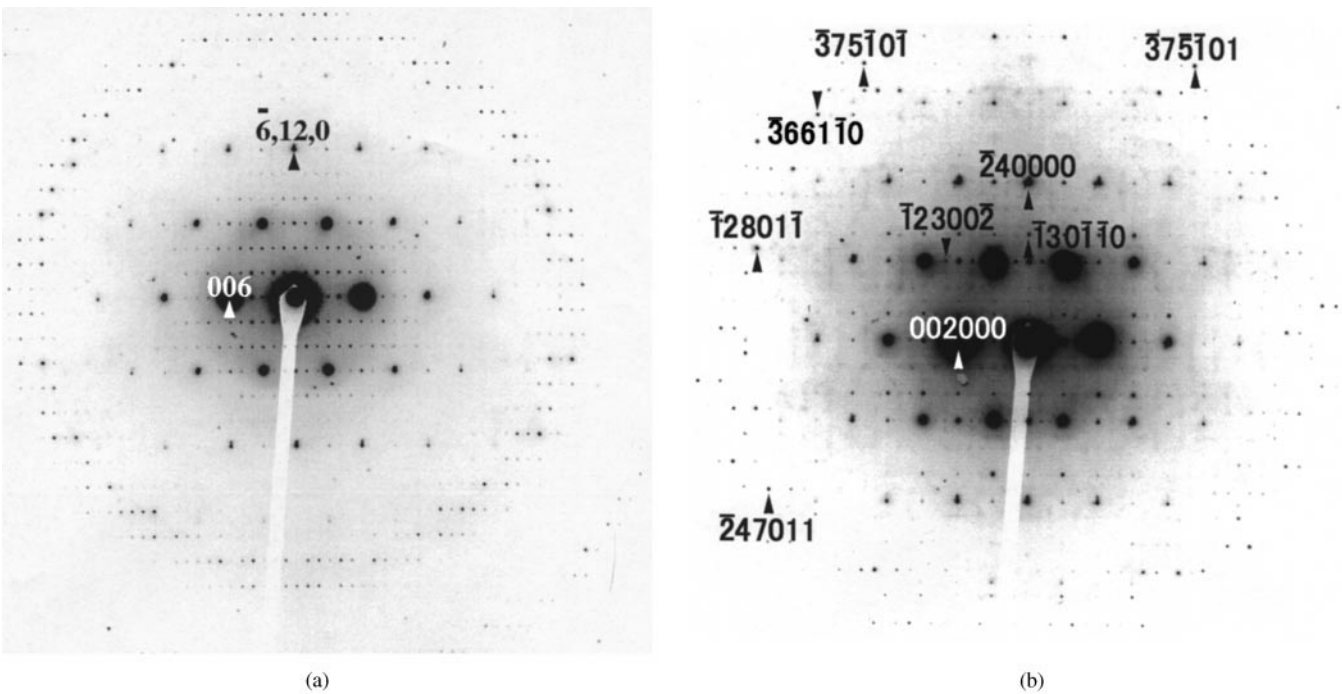

FIG. 5. Shows $\langle 210 \rangle$ zone axis EDPs typical of (a) the low-temperature $3 \times 3 \times 3$ superstructure phase and (b) the intermediate incommensurate phase. Indexation in (b) is with respect to the six basis vectors $\{\mathbf{a}^*, \mathbf{b}^*, \mathbf{c}^*, \mathbf{q}_1 = 0.31\mathbf{a}^*, \mathbf{q}_2 = 0.31\mathbf{b}^*, \mathbf{q}_3 = 0.31\mathbf{c}^*\}$. Note the simultaneous existence of all six $\mathbf{G} \pm 0.31\langle 110 \rangle^*$ type satellite reflections in (b) and the absence of higher order harmonic satellite reflections in (b) that are present in (a).

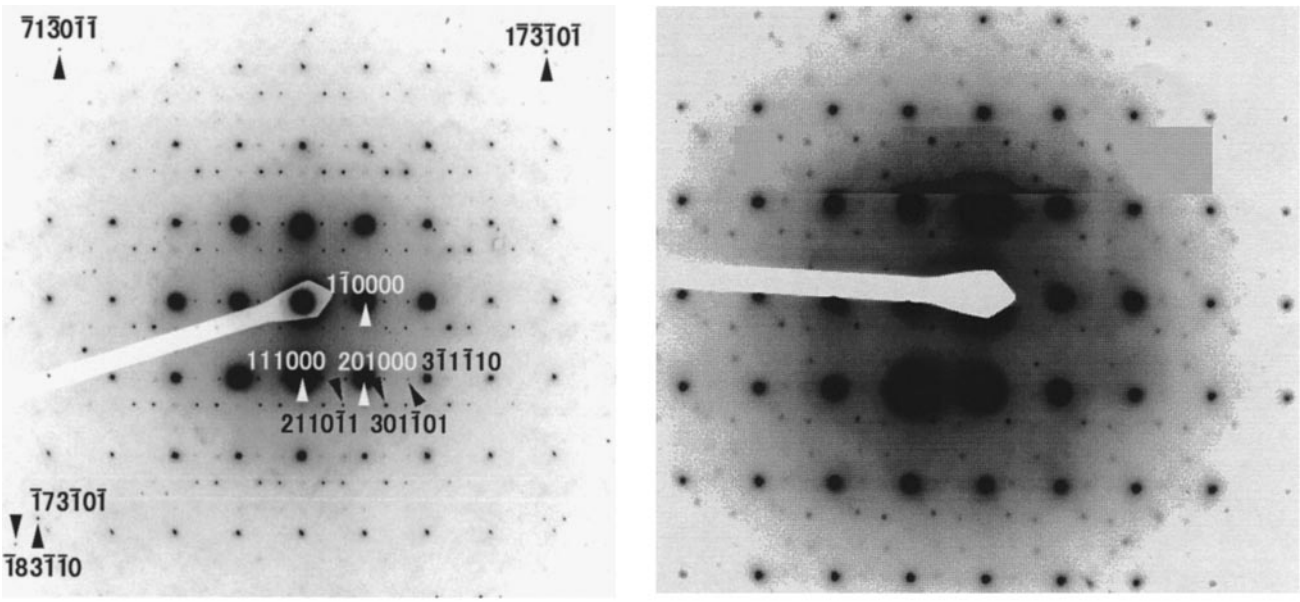

FIG. 6. Shows $\langle 11\bar{2}\rangle$ zone axis EDPs of the incommensurately modulated phases of (a) ZrP_2O_7 and (b) ZrV_2O_7. Indexation in (a) is with respect to the six basis vectors $\{\mathbf{a}^*, \mathbf{b}^*, \mathbf{c}^*, \mathbf{q}_1 = 0.31\mathbf{a}^*, \mathbf{q}_2 = 0.31\mathbf{b}^*, \mathbf{q}_3 = 0.31\mathbf{c}^*\}$. Note that the satellite reflections labeled $2110\bar{1}1$ and $301\bar{1}01$ in (b) are very slightly out of the plane of the ZOLZ as a result of the incommensurability (i.e., the deviation of 0.31 from $\frac{1}{3}$) but appear nonetheless as a result of the well-known shape transform effect.

given above, can be taken to be $\{-x_1 + \frac{1}{2},\ x_2 + \frac{1}{2},\ x_3,\ -x_4 + \frac{1}{2} + 2\phi_1,\ x_5 + \frac{1}{2},\ x_6\}$, $\{x_3,\ x_1,\ x_2,\ x_6 - (\phi_3 - \phi_1),\ x_4 - (\phi_1 - \phi_2),\ x_5 - (\phi_2 - \phi_3)\}$ and $\{-x_1,\ -x_2,\ -x_3,\ -x_4 + 2\phi_1,\ -x_5 + 2\phi_2,\ -x_6 + 2\phi_3\}$, respectively. At low temperature, when ε locks in to $\frac{1}{3}$ exactly, the resultant space group symmetry is determined by the choice of the three global phase parameters (17, 18) ϕ_1, ϕ_2, and ϕ_3, e.g., $Pa\bar{3}$ if $\phi_1 = \phi_2 = \phi_3 = 0$, $Pbca$ if $\phi_1 \neq \phi_2 \neq \phi_3 \neq 0$, $R\bar{3}$ if $\phi_1 = \phi_2 = \phi_3 \neq 0$, etc. The very existence of the intermediate incommensurate phase suggests that there is little free energy difference between these various possible choices of the global phase parameters. Difficulties in refining the low-temperature superstructure phase in such systems may well be associated with difficulties in refining the appropriate choice of global phases (17, 18).

4. DISCUSSION AND CONCLUSIONS

The existence of an intermediate incommensurately modulated phase, albeit of clearly different type, in the cases of both ZrP_2O_7 and ZrV_2O_7 raises the question as to whether such intermediate phases might be expected to occur in all $A^{IV}M_2^{V}O_7$ compounds that exhibit a low-temperature $3 \times 3 \times 3$ superstructure phase. The different symmetry of the intermediate incommensurate phases in the two cases is intriguing (and raises the possibility that the low-temperature $3 \times 3 \times 3$ superstructure phases in such systems need not necessarily be isomorphous).

There is certainly considerable evidence that there are a variety of distinct possible low-energy minima available for this structure type — DLS refinement, for example, gives a range of distinct possible structural minima (1–5). Presumably, the different relative sizes of the cations occupying the constituent octahedral and tetrahedral polyhedral units is responsible for altering the crystal chemical balance between the relative stiffnesses of the AO_6 octahedra and MO_4 tetrahedra in comparison to the energy gain associated with bending of the M–O–M bonds, thus also altering the nature of the intervening incommensurately modulated phase.

As the material "unfolds" due to thermal expansion upon heating, the P–O–P angles become (on average at least) closer to 180°, and the Zr–O–P angles must also approach some "average" value. As this happens, it seems very likely that the relative energies of the various different energy minima change. At some point different structures may become equivalent in energy. Instead of one simple modulation wave describing, e.g., the bending angles of the P–O–P units, the situation becomes far more complex. Clearly, there is much remaining to be understood about the crystallography and thermal expansion behavior of this fascinating class of materials.

ACKNOWLEDGMENTS

One of the authors (Y.T.) gratefully acknowledges the award of an Australian Research Council Post-doctoral Fellowship. We would like to thank the U.K. EPSRC for access to neutron diffraction facilities at the

ISIS facility of the Rutherford Appleton Laboratory and Dr. Richard Ibberson for assistance during data collection.

REFERENCES

1. V. Korthuis, N. Khosrovani, A. W. Sleight, N. Roberts, R.Dupree, and W. W. Warren, *Chem. Mater.* **7,** 412–417 (1995).
2. N. Khosrovani, V. Korthuis, A. W. Sleight, and T. Vogt, *Inorg. Chem.* **35,** 485–489 (1996).
3. N. Khosrovani, A. W. Sleight, and T. Vogt, *J. Solid State Chem.* **132,** 355–360 (1997).
4. J. S. O. Evans, J. C. Hanson, and A. W. Sleight, *Acta Crystallogr. B* **54,** 705–713 (1998).
5. A. W. Sleight, *Inorg. Chem.* **37,** 2854–2860 (1998).
6. H. Imomoto, H. Fukuoka, S. Tsunesawa, H. Horiuchi, T. Amemiya, and N. Koga, *Inorg. Chem.* **36,** 4172–4181 (1997).
7. A. K. A. Pryde, K. D. Hammonds, M. T. Dove, V. Heine, J. D. Gale, and M. C. Warren, *J. Phys.: Condens. Matter.* **8,** 10973–10982 (1996).
8. R. L. Withers, J. S. O. Evans, J. Hanson, and A. W. Sleight, *J. Solid State Chem.* **137,** 161–167 (1998).
9. G. L. Hua, T. R. Welberry, R. L. Withers, and J. G. Thompson, *J. Appl. Cryst.* **21,** 458–465 (1998).
10. R. L. Withers, J. G. Thompson, Y. Xiao, and R. J. Kirkpatrick, *Phys. Chem. Minerals* **21,** 421–433 (1994).
11. Y. Tabira, R. L. Withers, Y. Takeuchi, and F. Marumo, *Phys. Chem. Minerals* **27,** 194–202 (2000).
12. K. D. Hammonds, M. T. Dove, A. P. Giddy, and V. Heine, *Am. Miner.* **79,** 1207–1209 (1994).
13. M. T. Dove, V. Heine, K. D. Hammonds, M. Gambhir, and A. K. A. Pryde, *in* "Local Structure from Diffraction" (S. J. L. Billinge, and M. F.Thope, Eds.), pp. 253–271. Plenum, New York, 1998.
14. R. L. Withers, C. D. Ling, and S. Schmid, *Z. Kristallogr.* **214,** 296–304 (1999).
15. S. Esmaeilzadeh, P. Berastegui, J. Grins, and H. Rundlöf, *J. Solid State Chem.* **152,** 435–440 (2000).
16. S. Esmaeilzadeh, Ferroelectrics. (in press).
17. J. M. Pérez-Mato, *in* "Methods of Structural Analysis of Modulated Structures and Quasicrystals" (J. M. Pérez-Mato, F. J. Zúñiga, and G. Madariaga, Eds.), pp. 117–128. World Scientific, 1991.
18. R. L. Withers, S. Schmid, and J. G. Thompson, *Prog. Solid State Chem.* **26,** 1–96 (1998).